

Renal injury is a third hit promoting rapid development of adult polycystic kidney disease

Ayumi Takakura¹, Leah Contrino¹, Xiangzhi Zhou², Joseph V. Bonventre¹, Yanping Sun², Benjamin D. Humphreys¹ and Jing Zhou^{1,*}

¹Renal Division, Department of Medicine and ²Department of Radiology, Brigham and Women's Hospital and Harvard Medical School, 4 Blackfan Circle, Boston, MA 02115, USA

Received December 19, 2008; Revised and Accepted March 20, 2009

The 'two-hit' model is a widely accepted genetic mechanism for progressive cyst formation in autosomal dominant polycystic kidney disease. We have previously shown that adult inactivation of *Pkd1* using the *Mx1Cre*⁺ allele causes a late onset of focal cystic disease. An explanation for the delayed appearance of cysts is the requirement for an additional independent factor, or 'third hit'. Here we show that renal injury leads to massive cystic disease in the same mouse line. Cysts are labeled with a collecting duct/tubule marker, Lectin *Dolichos biflorus* Agglutinin, which correlates with the site of Cre-mediated recombination in the collecting system. 5-Bromo-2'-deoxyuridine labeling reveals that cyst-lining epithelial cells are comprised of regenerated cells in response to renal injury. These data demonstrate, for the first time, a role for polycystin-1 in kidney injury and repair and indicate that renal injury constitutes a 'third hit' resulting in rapid cyst formation in adulthood.

INTRODUCTION

Autosomal dominant polycystic kidney disease (ADPKD) is a common monogenetic disorder, occurring in 1:500 of the population (1,2). The disease results in end-stage renal disease in ~50% of subjects by the 6th decade. Mutations in the *PKD1* (85%) and *PKD2* (15%) genes, encoding polycystin-1 (PC1) and -2 (PC2) respectively, are responsible for this disease. Although every cell in ADPKD patients carries one germline mutated allele and one normal PKD allele, cyst formation occurs in only 5% of nephrons. The reasons for the focal nature of the disease are incompletely understood. However, the leading genetic hypothesis is a 'two-hit' model (3), which proposes that a germline mutation (first hit) in one allele of a PKD gene is not sufficient to result in cyst formation, but loss of both functional copies of a PKD gene upon a somatic mutation (second hit) later in life in a single cell is required for cyst formation. Germline homozygous deletion of *Pkd1* in mice results in numerous large cysts in kidney and pancreas during embryogenesis (4,5), indicating that *Pkd1* is necessary for normal kidney development and further supporting the 'two-hit' hypothesis. However, *Pkd1* inactivation induced in adult life, shown by us and

others, causes delayed cystogenesis (6–8). In our inducible *Pkd1* knockout (IKO) mouse model, which utilizes the *Cre/loxP* system and an interferon (IFN)-inducible *Mx1* promoter, inactivation of *Pkd1* in 1-week-old developing kidneys leads to rapid, widespread cyst formation in distal nephron segments, consistent with the 'two-hit' hypothesis. However, when *Pkd1* was inactivated in 5-week-old mice, there was only focal and slow progression of polycystic kidney disease (PKD). The discordance between rapid cyst growth in neonates versus much slower cyst growth in adult mice prompted us to search for a 'third hit', such as renal injury as a cause for rapid cyst development in adult life.

RESULTS

Renal ischemia–reperfusion injury causes extensive tubular damage in *Pkd1* IKO mice

To investigate the impact of loss of *Pkd1* on tubular injury, we performed unilateral renal ischemia reperfusion injury (IRI) on the *Pkd1* IKO and their littermate control mice. All mice were injected with polyinosinic-polycytidylic acid (pI:pC) to induce the expression of Cre recombinase and to inactivate *Pkd1* at

*To whom correspondence should be addressed at: Harvard Institutes of Medicine, Room 522, Brigham and Women's Hospital and Harvard Medical School 4 Blackfan Circle, Boston, MA 02115, USA. Tel: +1 6175255860; Fax: +1 6175255861; Email: zhou@rics.bwh.harvard.edu

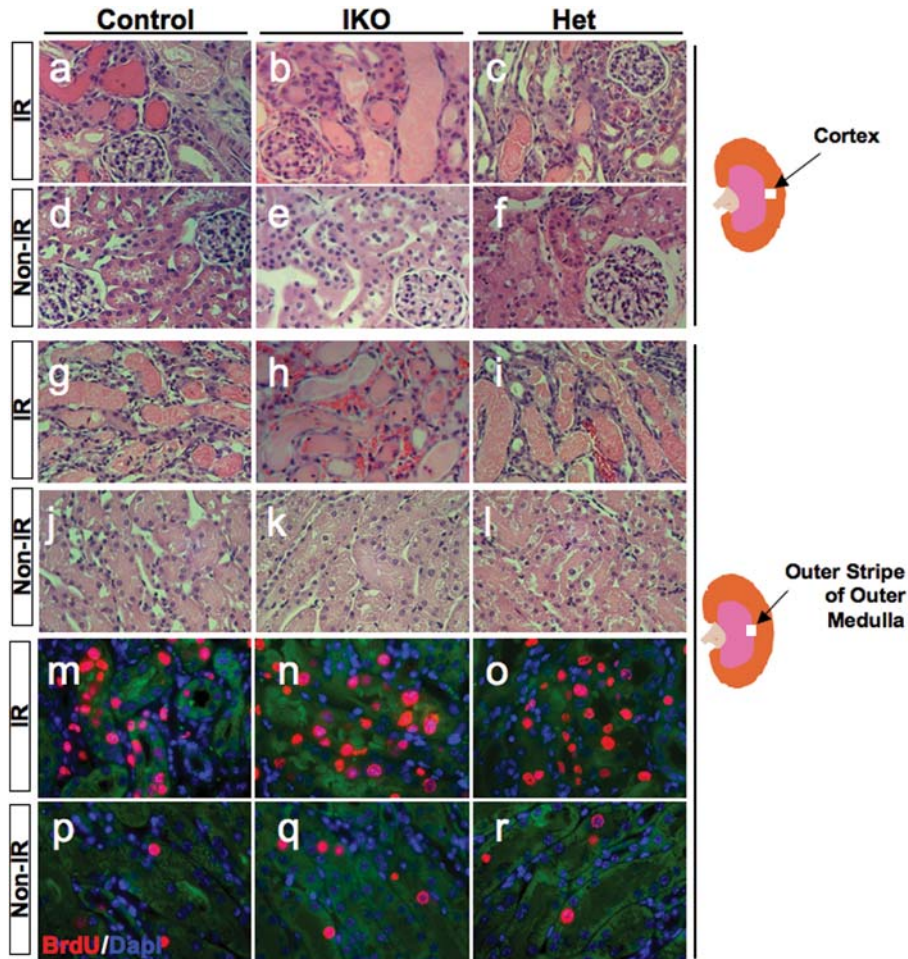


Figure 1. Extensive tubular damage and cell proliferation were seen in the renal corticomedullary junction response to ischemia–reperfusion injury. Sex-matched 5-week-old littermate mice were injected with pI:pC to induce Cre recombinase expression and subjected to IRI 4 weeks later. These mice were sacrificed 48 h after injury. Representative H&E staining of kidney sections were shown (a–l). Extensive tubular damage was seen in the renal corticomedullary junction in control (a, g), *Pkd1* IKO (b, h) and *Pkd1* heterozygous (c, i) mice. (d–f, g–i) Control kidney sections from not injured (non-IR) mice. Sections from ischemic kidney 48 h post-IRI (m–o) and contralateral non-ischemic kidneys (p–r) were labeled with anti-BrdU antibody (red). Autofluorescence (green) was used to illuminate the tubular structures. There is no significant difference in the number of BrdU-positive cells between control, *Pkd1* IKO and *Pkd1* heterozygous. The genotypes shown here are: control, *Pkd1*^{fllox/+}; IKO, *Mx1Cre*⁺*Pkd1*^{null/fllox}; Het, *Pkd1*^{null/+}.

5 weeks of age. Unilateral renal IRI was performed at 8 weeks of age. The mice were then sacrificed 48 h later. Extensive tubular damage including hyaline casts, epithelial cell detachment from the basement membrane, tubular dilatation and cellular cast formation were observed in both the inner cortex and the outer stripe of the outer medulla in the kidneys from all *Pkd1* IKO ($n = 10$), heterozygous *Pkd1*^{null/+} ($n = 5$) and littermate control ($n = 7$) mice, indicating successful IRI (Fig. 1A–C, G–I). As expected, contralateral (non-ischemic) kidneys were histologically normal (Fig. 1D–F, J–L). Interestingly, we found widespread and considerably more severe tubular damage in the inner stripe of outer medulla of *Pkd1* IKO kidneys (Fig. 2B) compared with littermate kidneys from mice without *Pkd1* inactivation (Fig. 2A). In contrast, contralateral (non-ischemic) kidneys were histologically normal in mice from all three genotypes (Fig. 2D–F). The inner stripe of the outer medulla contains distal straight tubules, descending thin limb of the loop of Henle and collecting ducts, and is not classically a site of severe injury in the

renal IRI model (9–11). Consistent with these results, heterozygous *Pkd1*^{null/+} kidneys showed slightly more severe tubular damage in the medulla, when compared with littermate kidneys from mice without *Pkd1* inactivation (Fig. 2C).

Renal ischemia–reperfusion injury causes extensive cell proliferation in *Pkd1* IKO mice

In contrast to adult kidney, the developing kidney is characterized by a very high rate of epithelial cell proliferation. Abnormal cell proliferation is also a major feature of cystic kidneys in ADPKD (12). Acute renal injury reactivates developmental signaling pathways and triggers epithelial cell proliferation (9,13). To verify that our model of unilateral, renal IRI causes cell proliferation, mice subjected to IRI were injected with 5-bromo-2'-deoxyuridine (BrdU) 48 h later, and were sacrificed 2 h after BrdU injection. BrdU incorporation, a measure of DNA synthesis, was visualized by immunohistochemistry. In agreement with previous studies (9), numerous

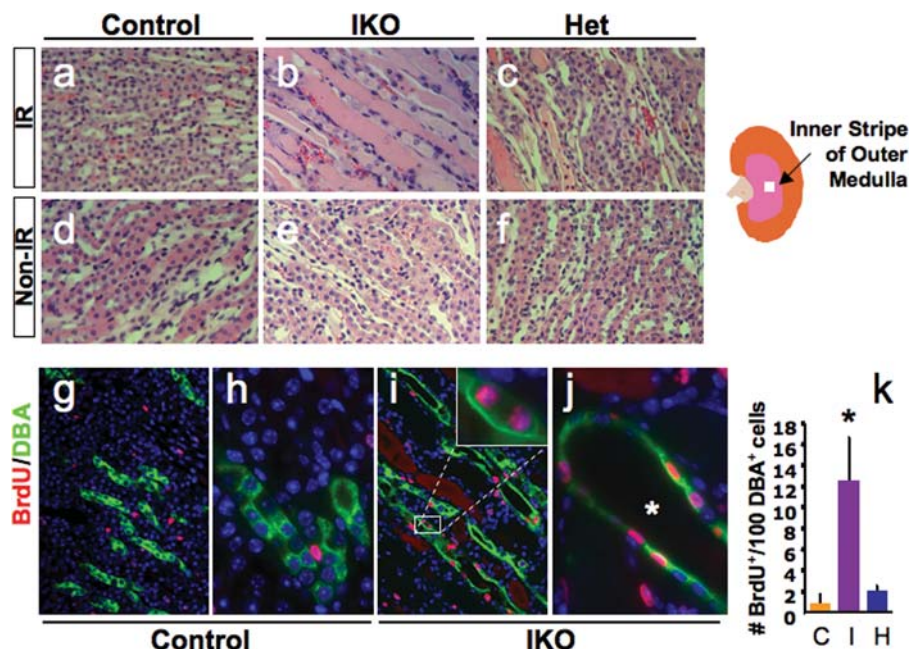


Figure 2. *Pkd1* IKO mice are susceptible to ischemia–reperfusion injury. Tubular damage in the inner stripe of outer medulla was significantly higher in *Pkd1* IKO mice (**b**) compared with control littermates (**a**, **c**). (**d–f**) Control kidney sections from not injured (non-IR) mice. (**g–j**) Sections were double labeled with anti-BrdU antibodies (red) and a collecting duct/tubule marker DBA (green). Compared with control mice (**g**, **h**), the number of BrdU-positive tubular epithelial cells (represented by DBA labeling) in medulla were higher in *Pkd1* IKO mice (**i**, **j**). Asterisk denotes dilated tubule (**k**). Quantitation of the number of BrdU-positive cells per hundred DBA-positive tubular epithelial cells in IKO mice. Data are mean \pm SD with three or four mice for each genotype group. * $P < 0.005$. C, control, I, IKO, H, Het.

BrdU-labeled cells were detected at the corticomedullary junction in injured kidneys from *Pkd1* IKO, heterozygous *Pkd1*^{null/+} and their littermate control mice (Fig. 1M–O), in contrast to the contralateral (non-ischemic) kidneys (Fig. 1P–R), indicating that renal IRI stimulus resulted in epithelial cell proliferation. Consistent with the more severe histological injury (Fig. 2B), we observed a significantly higher number of BrdU-labeled cells in tubules labeled with *Dolichos biflorus Agglutinin* (DBA), a collecting duct/tubule marker, in *Pkd1* IKO kidneys (Fig. 2I and J) compared with littermate control kidneys (Fig. 2G and H) (12.5 ± 4.1 versus 0.9 ± 0.9 BrdU⁺/100 DBA⁺ cells; $P < 0.005$) (Fig. 2G–K). There was a trend toward a higher number of BrdU-positive cells in heterozygous *Pkd1*^{null/+} kidney, when compared with control kidney, which did not reach statistical significance. These findings demonstrate that *Pkd1* inactivation in adult collecting tubules/ducts enhances susceptibility to ischemic injury.

Renal ischemia–reperfusion injury results in rapid cyst formation in *Pkd1* IKO mice

To determine whether renal IRI promotes cyst development, we subjected additional groups of animals to unilateral, renal IRI and allowed the kidney to repair. Small animal magnetic resonance imaging (MRI) was used to monitor cyst progression. Unilateral renal IRI was performed at 8 weeks of age (15 IKO and 12 control mice, Table 1). Sex-matched littermate heterozygous *Pkd1*^{null/+} mice ($n = 7$) were also included to determine the effect of *Pkd1* haploinsufficiency

Table 1. The total number of mice subjected to IRI

	IKO		Control		Het		Total
	m	f	m	f	m	f	
Unilateral IRI	18	19	14	16	6	4	77
Unilateral Sham	4	3	6	2	0	0	15
Bilateral IRI	3	3	3	3	0	2	14
Subtotal	25	25	23	21	6	6	106
Total	50		44		12		106

Note: m; male, f; female.

on cyst development. In stark contrast to the mice not subjected to injury (6), *Pkd1* IKO mice subjected to renal IRI developed multiple cysts that appear as light gray signals in the medulla of the injured kidneys 4 weeks later (Fig. 3B, left kidney, arrow). Cystic lesions were absent in the contralateral (non-ischemic) kidneys (Fig. 3B, right kidney, arrowhead) that served as an internal control. These experiments provide direct evidence that renal injury promotes cyst formation in mice with *Pkd1* inactivation induced in adult life. Importantly, kidneys from littermate control mice without *Pkd1* mutation did not develop cysts (Fig. 3A, C), ruling out the possibility that cyst development is simply a result of renal injury. While renal cysts were completely absent by MRI 6 weeks after renal injury in littermate control mice and only few cysts were observed in *Pkd1* IKO contralateral (non-ischemic) kidney (Supplementary Material, Fig. S1, arrowhead), a striking progression of renal cystic disease was evident in *Pkd1* IKO mice (Fig. 3E, Supplementary

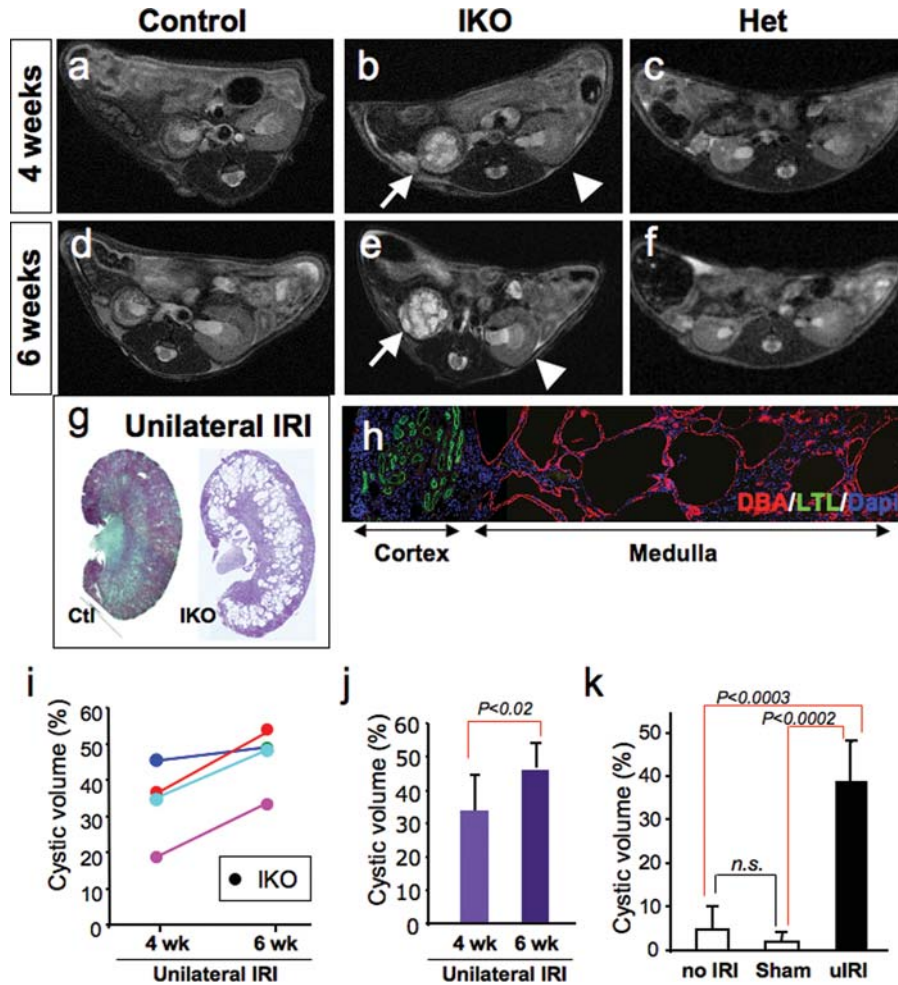


Figure 3. Unilateral ischemia reperfusion injury causes severe cystic disease in adult mice with *Pkd1* inactivation. Sex-matched 5-week-old littermate mice were injected with pI:pC and subjected to IRI 3 weeks later. Representative magnetic resonance imaging (MRI) images were taken at 4 (a–c) and 6 weeks (d–f) after unilateral IRI. No cysts were observed in *Pkd1*^{flx/flx} (control) (a, d) and *Pkd1*^{null/+} (Het) (c, f) mice. A striking polycystic phenotype is found in the ischemic kidney (arrow) but not in the contralateral (non-ischemic, arrowhead) kidney from *Mx1Cre*⁺*Pkd1*^{flx/flx} (IKO) mice (b, e). All mice shown here are males. *Mx1Cre*⁺*Pkd1*^{null/flx} (IKO) ischemic kidney sections were stained with DBA (red) and LTL (green) (h). Panels were digitally assembled to show the whole kidney and the cortex and medulla. The total cyst volume was measured in seven serial MRI images of injured kidneys from each of four *Pkd1* IKO mice at 4 and 6 weeks following IRI (i, j). The renal cyst volume of each of the four IKO mice (i) and their average (j) both indicate a steady rate of disease progression over 2 weeks. The total cyst volume was also measured in four serial H&E stained kidney sections from each of five injured (IRI), four not injured (no IRI) and three sham-operated (Sham) *Pkd1* IKO mice (k).

Material, Fig. S1). The presence of renal cysts detected by MRI was confirmed by H&E staining (Fig. 3G). Of note, only one out of seven heterozygous *Pkd1*^{null/+} mice showed a single cyst in the ischemic kidney, indicating that *Pkd1* inactivation in one allele is not sufficient to evoke extensive cystogenesis after renal injury. In contrast, contralateral kidneys were histologically normal but showed hypertrophy due to hyperfiltration (data not shown). Cysts in IKO mice after IRI were positive for a collecting duct/tubule marker, DBA but not for a proximal tubule marker, *Lotus tetragonolobus* lectin (LTL), which correlates with the site of Cre-mediated recombination in the collecting ducts/tubules for the *Mx1Cre* transgenic line (Fig. 3H). To determine the cyst volume, which we calculated it as the percentage of cystic area versus whole kidney area in a minimum of three sections,

MRI images of injured kidneys from four individual *Pkd1* IKO mice 4 and 6 weeks following IRI were analyzed using an imaging analysis software. The cyst volume of all four *Pkd1* IKO kidneys increased over the period (Fig. 3I and j, Table 2). To compare the severity of PKD between the injured, not injured and sham-operated *Pkd1* IKO mice, we determined the cyst volume in four H&E-stained sections of 14-week-old kidneys from each of 12 IKO mice and found a dramatic increase in cyst volume in the injured *Pkd1* IKO kidneys 6 weeks following IRI (Fig. 3K). To investigate the time course of cystogenesis in response to IRI, we dissected mice 1 and 2 week(s) after IRI. Tubule dilatation was observed as early as 1 week after IRI and widespread small cysts were detected after another week (Supplementary Material, Fig. S2). To verify the findings in unilateral IRI model, we

Table 2. The time course of cyst volume (%) in *Pkd1* IKO kidneys after IRI

Unilateral IRI	4 week	6 week	Bilateral IRI	2 week	5 week	11 week
IKO			IKO			
Mouse 1	35.60	48.58	Mouse 1	6.55	23.94	42.38
Mouse 2	19.08	34.01	Mouse 2	7.75	29.85	50.58
Mouse 3	44.41	47.86	Mouse 3	5.29	42.38	64.2
Mouse 4	35.95	52.81				
Cyst volume (%) Mean \pm SD	33.76 \pm 10.60	45.81 \pm 8.17	Cyst volume (%) Mean \pm SD	6.53 \pm 1.23	32.06 \pm 9.41	52.39 \pm 11.02

Note: Unilateral IRI; $P = 0.014$ for 4 versus 6 week. Bilateral IRI; $P = 0.025$ for 2 versus 5 week, $P = 0.0012$ for 5 versus 11 week, $P = 0.011$ for 2 versus 11 week. Cyst volume, percentage of cystic area versus total kidney area.

performed bilateral renal IRI on *Pkd1* IKO or control mice. As expected, the progression of PKD in *Pkd1* IKO kidneys can be detected by MRI at 2 (Fig. 4B), 5 (Fig. 4E) and 11 weeks (Fig. 4H) after bilateral IRI. Only *Pkd1* IKO mice ($n = 6$) developed extensive cyst formation in both kidneys (Fig. 4B, E, H), in comparison with littermate non-IKO control ($n = 5$) or heterozygous *Pkd1*^{null/+} mice ($n = 2$). Severe renal cystic disease in *Pkd1* IKO kidney can also be seen by histology (Fig. 4I). Similar to human ADPKD, *Pkd1* IKO mice exhibited massively enlarged kidney, compared with control kidneys (Fig. 4J). Analyses of a total of 54 MRI images from both kidneys of three *Pkd1* IKO mice at 2, 5 and 11 weeks following bilateral IRI revealed that there is a remarkable increase (~ 8 -fold) in cyst volume in the *Pkd1* IKO kidneys in the 9-week period we investigated (Fig. 4K and L, Table 2).

Cell proliferation in response to renal injury is increased in *Pkd1* IKO mice

Recent studies show that repairing cells in the kidney in response to IRI derive from proliferation of surviving tubular epithelial cells (14). To explore the role of epithelial cell proliferation on injury-induced cystogenesis and to determine whether cyst-lining epithelial cells are comprised of regenerated cells after kidney injury, we injected BrdU on the 2nd and 3rd days after unilateral IRI to label proliferating cells. Nine weeks later, kidneys were harvested and the paraffin-embedded kidney sections were co-stained with anti-BrdU antibody and DBA. The intensity of BrdU labeling in DBA-positive cyst-lining epithelial cells and dilated tubules in IKO mice was weak, and barely detectable in some cysts (Fig. 5A and B), which is in marked contrast to the strong signals observed at 48 h post-IRI (Fig. 5C), suggesting a dilution of BrdU following multiple rounds of cell proliferation. This set of experiments suggests that cyst-lining cells are derived from tubular epithelia that have proliferated in response to IRI (14). To investigate the time course of cell proliferation in collecting ducts/tubules in response to IRI, kidney sections were co-stained with an antibody against Ki67, a cell proliferation marker, and the collecting duct/tubule marker DBA. Approximately 900 DBA-labeled cells in six non-overlapping areas of two kidney sections from each of three experimental and three control mice were counted for Ki67 at four time points [48 h, 1, 2 and 7 week(s)]. We defined the percentage of Ki67 and DBA double-labeled cells versus

total of DBA-labeled cells as tubular cell proliferation index (tPI). In injured kidney from *Pkd1* IKO mice, about 60% of collecting ducts/tubules were positively labeled for Ki67 48 h after IRI and this population dropped by $\sim 50\%$ 1 week after IRI (Fig. 5D, Table 3). Compared with control mice, IKO mice tend to display a higher tPI at 48 h after IRI, but did not reach statistical significance. A significant increase in tPI was seen, however, in *Pkd1* IKO kidney at 1 week ($\sim 28\%$) and 2 weeks ($\sim 21\%$) after IRI when small cysts are widespread (Supplementary Material, Fig. S2). The tubular proliferation index remained at $\sim 9\%$ in *Pkd1* IKO kidneys 7 weeks after IRI (Fig. 5D, Table 3). In contrast, injured kidney from control mice without *Pkd1* inactivation had no Ki67 positive cells at these stages (Fig. 5D, Table 3).

DISCUSSION

Because adult inactivation of *Pkd1* in the kidney results in only focal and late onset of PKD, we recently proposed the 'third hit' hypothesis for ADPKD (6). Here we have tested renal IRI as a 'third hit' to cause rapid cyst development in adult life.

Two days after renal IRI we observed extensive tubular damage in both the inner cortex and the outer stripe of the outer medulla in the kidneys from all *Pkd1* IKO, heterozygous *Pkd1*^{null/+}, and littermate control mice. However, *Pkd1* IKO mice exhibited widespread and more severe tubular damage in the inner stripe of outer medulla in kidneys, where *Mx1*Cre-mediated recombination (*Pkd1* inactivation) takes place in this mouse line. The data suggest that *Pkd1* expression normally protects these nephron segments from ischemic injury. *Pkd1* may act either to protect tubular epithelia from injury or to accelerate repair, or both.

To see whether injury-induced cell proliferation in *Pkd1* IKO kidney leads to cyst formation, we monitored the progression of PKD by MRI. In contrast to the contralateral (non-ischemic) kidney of *Pkd1* IKO mice that served as an internal control, *Pkd1* IKO injured kidney developed severe widespread cystic disease. To verify this observation after unilateral IRI, we performed bilateral IRI on *Pkd1* IKO mice. As expected, *Pkd1* IKO mice exhibited massively enlarged polycystic kidneys. Our study clearly demonstrates that IRI promotes renal cyst formation in cells that have received 'two hits' in *Pkd1*. Defects of primary cilia are implicated in the pathogenesis of PKD (15) and that PC1-deficient cells cannot respond to fluid flow shear stress

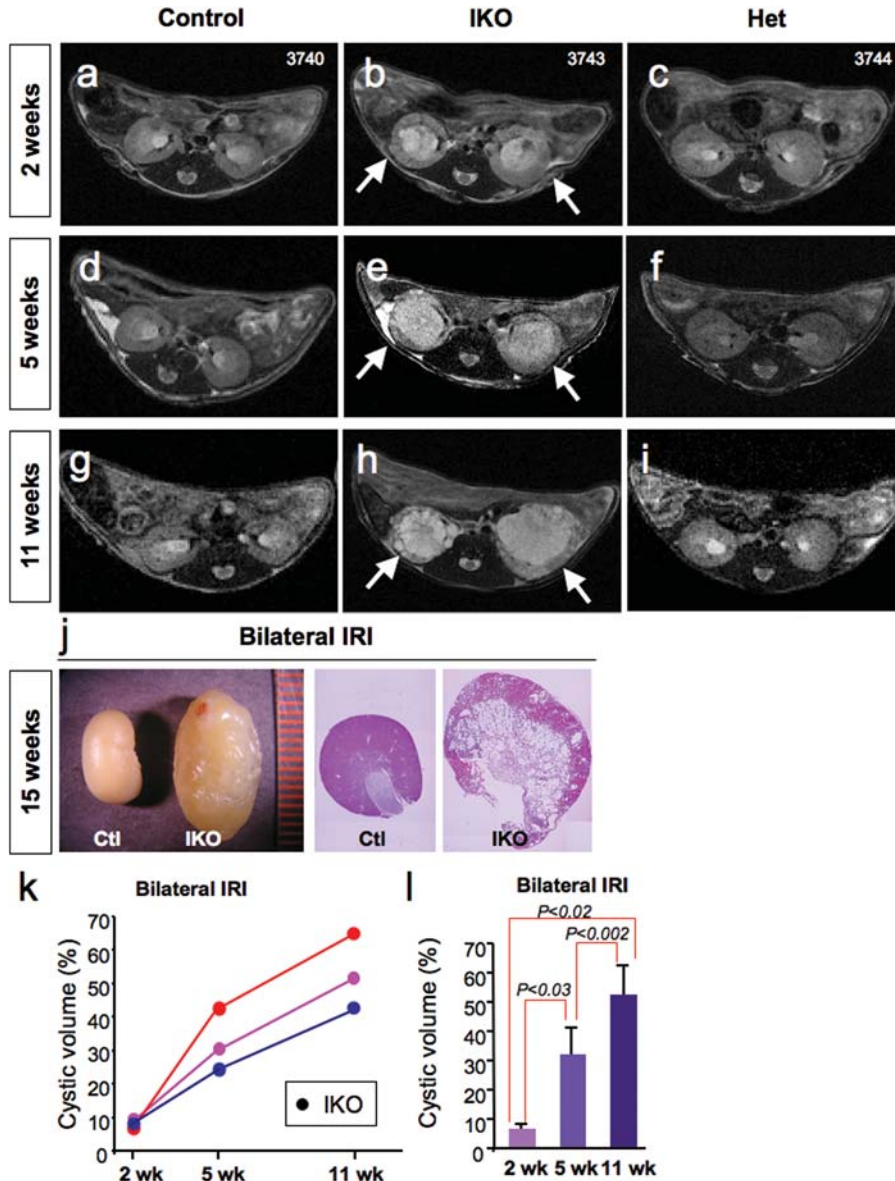


Figure 4. The enlargement of polycystic kidney is accelerated in response to bilateral ischemia–reperfusion injury. Representative MRI images were taken at 2 (a–c), 5 weeks (d–f) and 11 weeks (g–i) after bilateral IRI. The progression of polycystic phenotype was observed in the both ischemic kidneys (arrows) in *Pkd1* IKO mice, while the injured kidneys in their littermate control and *Pkd1*^{null/+} mice were recovered from injury. (j) Gross appearance of massively enlarged polycystic (right) and normal (left) kidneys from respective IKO and control mice 15 weeks after bilateral IRI. Representative H&E staining sections of these kidneys are shown in the right panels. The cyst volume was measured in six independent MRI images of both kidneys from each of three *Pkd1* IKO mice at 2, 5 and 11 weeks following IRI (k, l). The cyst volume in each mouse ($n = 3$) (k) and the average cystic volume of a *Pkd1* IKO kidney ($n = 6$) (l) steadily increase with time.

through their primary cilia (16). Recently, Patel *et al.* (17) reported that adult *Kif3A* knockout mice exhibit mild cystic phenotype 2.5 weeks after 45 min of ischemia followed by reperfusion. In our mouse model, widespread small cysts were observed as early as 2 weeks after 25 min of ischemia followed by reperfusion, which is a milder ischemic condition. It is noteworthy that the nephron segments developing cystic lesions are collecting ducts/tubules in our *Pkd1* model, and proximal tubule and thick ascending limbs of the loops of Henle in the *Kif3a* model. One possible explanation for the difference in phenotype is that the role of PC1 in adult

collecting tubules/ducts in the kidney is either cilia independent or PC1 may serve more functions than a mechanosensor on primary cilia. However, further studies are required to address the role of PC1 on cilia in adult life because the Cre recombinase used to inactivate *Pkd1* and *Kif3a* in these two studies was driven under different tissue-specific promoters (*Mx1* and *Ksp*, respectively), which may have different activity in specific nephron segments. Nevertheless, we have established an excellent animal model for PKD1-disease that accounts for ~85% of human ADPKD cases.

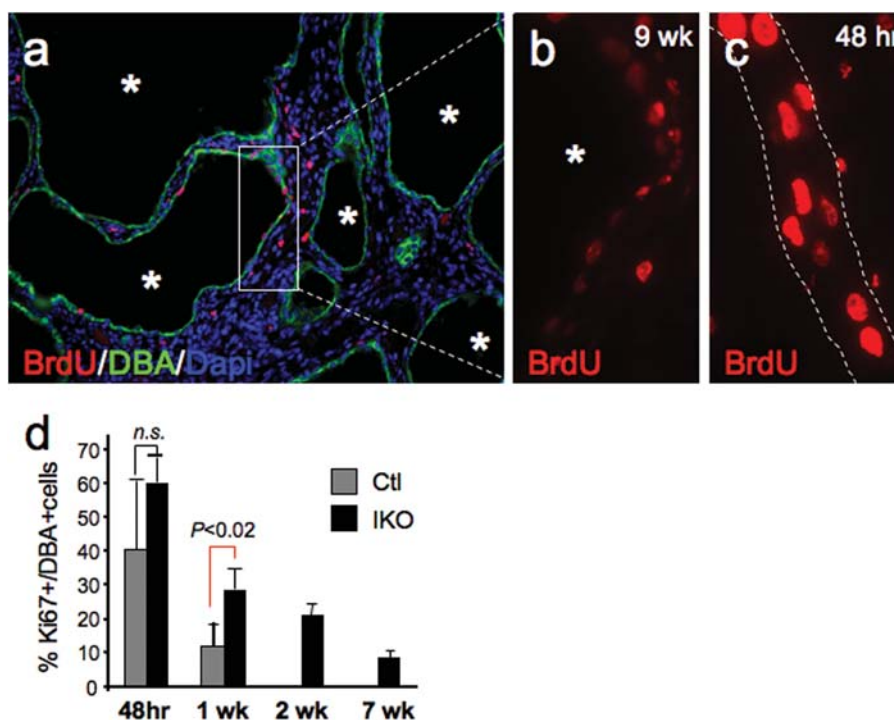


Figure 5. Cell proliferation in *Pkd1* IKO kidneys post-IRI. (a–c) Kidney sections were double labeled with anti-BrdU antibody (red) and DBA (green). Diluted BrdU signals were detected in cyst-lining epithelial cells in IKO mice 9 weeks after IRI (a, b), in contrast to the strong BrdU signals at 48 h after IRI (c). Dashed lines outline the tubule in (c). Photos were taken under the same exposure time for (b) and (c). The tubular cell proliferation index (percentage of Ki67 positive cells in DBA positive cells) was measured in six non-overlapping areas of two kidney sections from each of three experimental and three control mice at 48 h, 1, 2 and 7 week(s) following IRI (d).

Table 3. The time course of tubular proliferation index (%) in *Pkd1* IKO kidneys after IRI

	48 h			1 week			2 week			7 week		
	Ki67	DAPI-DBA	tPI (%)	Ki67	DAPI-DBA	tPI (%)	Ki67	DAPI-DBA	tPI (%)	Ki67	DAPI-DBA	tPI (%)
Control												
Mouse 1	78	430	18.1	130	830	15.66	0	>500	0	0	>500	0
Mouse 2	439	754	58.2	83	520	15.96	0	>500	0	0	>500	0
Mouse 3	308	681	45.2	27	589	4.58	0	>500	0	0	>500	0
Total cells counted	825	1865		240	1939		0	>1500		0	>1500	
Mean \pm SD (%)			40.53 \pm 20.45			12.07 \pm 6.48			0			0
IKO												
Mouse 1	384	655		422	1186	35.58	174	986	17.65	123	1128	10.9
Mouse 2	305	575		222	886	25.06	228	1086	20.99	79	822	8.39
Mouse 3	726	1066		328	1306	25.11	561	2289	24.51	43	676	6.36
Total cells counted	1415	2296		972	3378		963	5361		235	2626	
Mean \pm SD (%)			59.92 \pm 7.61			28.58 \pm 6.06			21.05 \pm 3.43			8.55 \pm 2.28

Note: Tubular cell proliferation index (tPI), percentage of the number of Ki67 positive cells in DBA positive tubular epithelial cells.

The mechanism(s) for injury-induced cystogenesis in *Pkd1* IKO mice is unknown. It is possible that *Pkd1*-deficient cells, unlike normal tubular epithelial cells, fail to switch off the normal renal injury-induced repair program. Instead, they continue to proliferate, resulting in cyst formation. The BrdU tracing study revealed that BrdU-incorporated cells in response to IRI in *Pkd1* IKO kidney continue to proliferate. Consistent with this finding, the tubular proliferation index

in collecting ducts/tubules fail to reduce to baseline after IRI. These results, in contrast to a recent report (8), support the classic model that increased cell proliferation is a major requirement of cyst development in human ADPKD (12). Notably the number of Ki67 positive cells in *Pkd1* IKO kidney was similar to that in littermate control kidney 48 h after IRI despite the BrdU-labeled cells were significantly higher in *Pkd1* IKO kidney. BrdU incorporation occurs

during DNA synthesis in S phase, whereas Ki67 is expressed in all phases of the cell cycle (G1, S, G2, M). The Ki67-positive cells in collecting ducts/tubules in the injured wild-type kidneys may not be actively cycling because distal nephron segments including collecting tubules are not usually affected by IRI, in contrast to the S3 segment of the proximal tubule (9–11). Accordingly, we speculate that polycystin-1 may regulate G1 to S transition in mature renal epithelial cells. When PC1 is disrupted, distal tubular epithelial cells entering G1 phase as a response to injury will proceed to S phase, and the cell cycle progresses. An alternative explanation is that there is a defect in the control of the length of S phase in *Pkd1* IKO kidney, such as a prolonged S phase that contributes to the increase in BrdU-labeled cells. Overall, these data suggested that tubular epithelial cells with *Pkd1* inactivation have enhanced susceptibility to injury.

The data reported here provide the first experimental evidence supporting the ‘third hit’ hypothesis that renal injury or other genetic or non-genetic insults reactivating developmental programs and/or increasing cell proliferation promotes rapid cyst formation in mature kidneys in a orthologous model of human cystic disease. Several cross-sectional studies including the CRISP study have demonstrated considerable heterogeneity in the size of cysts within and between human ADPKD kidneys (18). Results from the current study suggest that in humans with ADPKD, subclinical kidney injury may be an important factor determining disease progression in adults. Preventing kidney injury and targeting the developmental pathways reactivated in repairing kidney represent important areas of possible intervention in the at risk population.

MATERIALS AND METHODS

Generation of inducible *Pkd1* knockout mice

Inducible *Pkd1* knockout mice were generated by crossing *Pkd1*^{flox/+} mice with a transgenic mouse line that expresses Cre recombinase under the control of an interferon-inducible *Mx1* promoter (*Mx1Cre* mice). The resultant *Mx1Cre*⁺*Pkd1*^{flox/+} mice were bred with either *Pkd1*^{flox/+} mice or *Pkd1*^{null/+} mice to generate *Mx1Cre*⁺*Pkd1*^{flox/flox} mice or *Mx1Cre*⁺*Pkd1*^{null/flox} mice, respectively. *Pkd1*^{flox/+}, *Pkd1*^{flox/flox} or *Mx1Cre*⁺*Pkd1*^{+/+} mice were used as controls, and *Pkd1*^{null/flox}, *Pkd1*^{null/+} or *Mx1Cre*⁺*Pkd1*^{null/+} mice were used as heterozygous *Pkd1*^{null/+}.

Induction of Cre expression

Mice were intraperitoneally injected with 250 µg of IFN inducer pI:pC (Sigma) for 5 consecutive days at 5 weeks of age to induce the expression of Cre recombinase.

Renal IRI model

Studies were performed according to the animal experimental guidelines issued by the Animal Care and Use Committee at Harvard University. Animals were anesthetized with pentobarbital sodium (60 mg/kg body weight, intraperitoneally) prior

to surgery. Body temperatures were controlled at 36.5–37.5°C throughout the procedure. Kidneys were exposed through flank incisions, and mice were subjected to ischemia by clamping the left renal pedicle or both left and right renal pedicle with nontraumatic microaneurysm clamps (Roboz, Rockville, MD, USA), which were removed after 25 min (males) or 35 min (females). One milliliter of 0.9% NaCl was administered subcutaneously 2 h after surgery. Sham operation was done in the same manner but without clamping of the renal pedicles. To label proliferating cells, mice were injected with BrdU (Sigma-Aldrich) intraperitoneally (50 mg/kg body wt) 48 h after IRI, and sacrificed 2 h later. Some mice were injected with BrdU on the 2nd and 3rd days after IRI and sacrificed more than 5 weeks after surgery.

Histology and immunohistochemistry

Paraffin-embedded sections (4 µm) were dewaxed, rehydrated through graded alcohols and boiled in 10 mM citrate (pH 6.0) (VECTOR) for 30 min. The sections were then placed in the staining dish at room temperature and allowed to cool for 1–2 h. Sections were incubated with 10% goat serum for 30 min and incubated with anti-BrdU antibody (1:100, BD Biosciences) or Ki67 (1:100, Vector) overnight at 4°C or for 1 h at room temperature. After washing with PBS, sections were incubated with secondary antibody for 1 h at room temperature. For double staining with tubules markers, Lectin DBA (VECTOR) and *Lotus Tetragonolobus Lectin* (LTL) (VECTOR), a dilution of 1:500 was used. After washing with PBS, sections were mounted with Prolong Gold antifade reagent with DAPI (Invitrogen).

MRI experiments

MRI measurements were performed with a 4.7 T Bruker Avance horizontal bore system. The mice were anesthetized with 1% isoflurane in an oxygen mixture. After the mouse was fully anesthetized, the entire mouse was then placed in a special home-made body holder in order to minimize motion artifacts. Animals were imaged with a RARE imaging sequence (TR = 2800 ms, effective TE = 55 ms) in the coronal plane with a slice thickness of 0.75 mm and a slice number sufficient to both kidneys, with a matrix size of 256 × 192 and field of view of 3 × 3 cm².

Measurement of cyst volume

The cyst volume was quantified in whole kidney sections using Image Pro Plus v5 software (Media Cybernetics) and calculated as (cystic area/total kidney area) × 100%. In MRI images of unilateral IRI kidneys, seven sections per kidney at each time point were analyzed for each mouse. In MRI images of bilateral IRI kidneys, three sections for each kidney and each time point were analyzed for each mouse. In H&E staining sections, four sections were analyzed for each mouse.

Tubular cell proliferation index

The tPI was measured by counting Ki67-positive cells in DBA-positive tubular epithelial cells and calculated as the percentage of Ki67 and DBA double-labeled cells versus total DBA-labeled cells. Six non-overlapping areas of two kidney sections at each time point were analyzed for each mouse.

Statistic analysis

The significance of differences between groups was determined by Student's *t*-test. A *P*-value of <0.05 was considered statistically significant.

SUPPLEMENTARY MATERIAL

Supplementary Material is available at *HMG* online.

ACKNOWLEDGEMENTS

The authors would like to thank Dr. Kambiz Zandi-Nejad for assistance in manuscript preparation and scientific suggestions. The authors also thank Drs Patrick Starremans, Jordan Kreidberg and other members of the Polycystic Kidney Disease Center at several Harvard institutions for scientific discussions and support.

Conflict of Interest statement. None declared.

FUNDING

This work was supported by grants from the National Institutes of Health (DK51050 and DK40703) to J.Z., DK73628 to B.H. and DK074030 to the Harvard Center of Polycystic Kidney Disease. A.T. was a recipient of a postdoctoral fellowship from the American Heart Association.

REFERENCES

- Zhou, J. and Pei, Y. (2007) Autosomal dominant polycystic kidney disease. *Elsevier*, 85–171.
- Zhou, J. (2009) Polycystins and primary cilia, primers for cell cycle progression. *Ann. Rev. Physiol.*, **71**, 83–113.
- Reeders, S.T. (1992) Multilocus polycystic disease. *Nat. Genet.*, **1**, 235–237.
- Lu, W., Shen, X., Pavlova, A., Lakkis, M., Ward, C.J., Pritchard, L., Harris, P.C., Genest, D.R., Perez-Atayde, A.R. and Zhou, J. (2001) Comparison of Pkd1-targeted mutants reveals that loss of polycystin-1 causes cystogenesis and bone defects. *Hum. Mol. Genet.*, **10**, 2385–2396.
- Lu, W., Peissel, B., Babakhanlou, H., Pavlova, A., Geng, L., Fan, X., Larson, C., Brent, G. and Zhou, J. (1997) Perinatal lethality with kidney and pancreas defects in mice with a targeted Pkd1 mutation. *Nat. Genet.*, **17**, 179–181.
- Takakura, A., Contrino, L., Beck, A.W. and Zhou, J. (2008) Pkd1 inactivation induced in adulthood produces focal cystic disease. *J. Am. Soc. Nephrol.*, **19**, 2351–2363.
- Lantinga-van Leeuwen, I.S., Leonhard, W.N., van der Wal, A., Breuning, M.H., de Heer, E. and Peters, D.J. (2007) Kidney-specific inactivation of the Pkd1 gene induces rapid cyst formation in developing kidneys and a slow onset of disease in adult mice. *Hum. Mol. Genet.*, **16**, 3188–3196.
- Piontek, K., Menezes, L.F., Garcia-Gonzalez, M.A., Huso, D.L. and Germino, G.G. (2007) A critical developmental switch defines the kinetics of kidney cyst formation after loss of Pkd1. *Nat. Med.*, **13**, 1490–1495.
- Witzgall, R., Brown, D., Schwarz, C. and Bonventre, J.V. (1994) Localization of proliferating cell nuclear antigen, vimentin, c-Fos, and clusterin in the postischemic kidney. Evidence for a heterogeneous genetic response among nephron segments, and a large pool of mitotically active and dedifferentiated cells. *J. Clin. Invest.*, **93**, 2175–2188.
- Bonventre, J.V. (1988) Mediators of ischemic renal injury. *Annu Rev Med.*, **39**, 531–544.
- Bonventre, J.V. (2003) Dedifferentiation and proliferation of surviving epithelial cells in acute renal failure. *J. Am. Soc. Nephrol.*, **14** (Suppl 1), S55–S61.
- Grantham, J.J., Geiser, J.L. and Evan, A.P. (1987) Cyst formation and growth in autosomal dominant polycystic kidney disease. *Kidney Int.*, **31**, 1145–1152.
- Villanueva, S., Cespedes, C. and Vio, C.P. (2006) Ischemic acute renal failure induces the expression of a wide range of nephrogenic proteins. *Am. J. Physiol. Regul. Integr. Comp. Physiol.*, **290**, R861–R870.
- Humphreys, B.D., Valerius, M.T., Kobayashi, A., Mugford, J.W., Soeung, S., Duffield, J.S., McMahon, A.P. and Bonventre, J.V. (2008) Intrinsic epithelial cells repair the kidney after injury. *Cell Stem Cell*, **2**, 284–291.
- Lin, F., Hiesberger, T., Cordes, K., Sinclair, A.M., Goldstein, L.S., Somlo, S. and Igarashi, P. (2003) Kidney-specific inactivation of the KIF3A subunit of kinesin-II inhibits renal ciliogenesis and produces polycystic kidney disease. *Proc. Natl Acad. Sci. USA*, **100**, 5286–5291.
- Nauli, S.M., Alenghat, F.J., Luo, Y., Williams, E., Vassilev, P., Li, X., Elia, A.E., Lu, W., Brown, E.M., Quinn, S.J. *et al.* (2003) Polycystins 1 and 2 mediate mechanosensation in the primary cilium of kidney cells. *Nat. Genet.*, **33**, 129–137.
- Patel, V., Li, L., Cobo-Stark, P., Shao, X., Somlo, S., Lin, F. and Igarashi, P. (2008) Acute kidney injury and aberrant planar cell polarity induce cyst formation in mice lacking renal cilia. *Hum. Mol. Genet.*, **17**, 1578–1590.
- Grantham, J.J., Torres, V.E., Chapman, A.B., Guay-Woodford, L.M., Bae, K.T., King, B.F. Jr, Wetzel, L.H., Baumgarten, D.A., Kenney, P.J., Harris, P.C. *et al.* (2006) Volume progression in polycystic kidney disease. *N. Engl. J. Med.*, **354**, 2122–2130.